Received: 21 August 2018 | Revised: 3 May 2019 | Accepted: 11 June 2019

DOI: 10.1002/joc.6201

RESEARCH ARTICLE

International Journal of Climatology RMetS

Anticipated changes to the snow season in Alaska: Elevation dependency, timing and extremes

Rick Lader[1,2] | **John E. Walsh**[2] | **Uma S. Bhatt**[1] | **Peter A. Bieniek**[2]

[1]Department of Atmospheric Sciences, Geophysical Institute, University of Alaska Fairbanks, Fairbanks, Alaska

[2]International Arctic Research Center, University of Alaska Fairbanks, Fairbanks, Alaska

Correspondence
Rick Lader, International Arctic Research Center, University of Alaska Fairbanks, P.O. Box 752325, Fairbanks, AK 99775.
Email: rtladerjr@alaska.edu

Funding information
United States Geological Survey, Grant/Award Number: G17AC00213; NOAA Climate Program Office, Grant/Award Number: NA16OAR4310162; Office of Polar Programs, Grant/Award Number: PLR-1268350; National Science Foundation

Abstract

Snowfall and snow season length across Alaska control the surface hydrology and underlying soil properties and also influence near-surface air temperature by changing the energy balance. Current projections of warming suggest that considerable change will occur to key snow parameters, possibly contributing to extensive infrastructure damage from thawing permafrost, an increased frequency of rain-on-snow events and reduced soil recharge in the spring due to shallow end-of-winter snowpack. This study investigates projected changes to mean annual snowfall, dates of snow onset and snowmelt and extreme snowfall for Alaska, using dynamically downscaled reanalysis and climate model simulations. These include the ERA-Interim reanalysis from 1981 to 2010, and two Coupled Model Intercomparison Project Phase 5 models: Community Climate System Model version 4 (CCSM4) and Geophysical Fluid Dynamics Laboratory Climate Model version 3 (GFDL-CM3) from 1981 to 2100. The analysis is presented in 30-year periods (i.e., 1981–2010, 2011–2040, 2041–2070 and 2071–2100) with the future scenarios from Representative Concentration Pathway 8.5. Late-century projections of average annual snowfall at low elevations (0–1,000 m) show decreases of 41.3 and 40.6% for CCSM4 and GFDL-CM3, respectively. At high elevations (1,000–2,000 m), the reductions are smaller at 13.5 and 14.2%, respectively. End-of-winter snow-water equivalent displays reductions at all elevations in the future periods. Snow season length is shortened due to later snow onset and earlier snowmelt; many locations in southwest Alaska no longer experience continuous winter snowpack by the late-century period. Maximum 2-day snowfall amounts are projected to decrease near Anchorage and Nome, while Fairbanks and Utqiaġvik (Barrow) show no significant trend.

KEYWORDS

Alaska, Arctic climate, dynamical downscaling, extremes, snowfall

1 | INTRODUCTION

Snow cover and snowfall are prominent features of the climate of Alaska that help regulate surface temperature and physical attributes of the near-surface soil. With its high albedo, snow reflects solar energy back toward space, and deeper snow cover tends to have a higher albedo (Hall, 2004). However, in the context of rising greenhouse gas concentrations, this snow-albedo feedback has contributed to a rate of surface warming in the Arctic that is nearly

 © 2019 Royal Meteorological Society

double the global average during the most recent decades (Overland *et al.,* 2016; AMAP, 2017). Studies of Northern Hemisphere snow cover extent and snow season duration indicate large reductions that are most severe in the spring (Brown and Robinson, 2011; IPCC, 2013; Estilow *et al.,* 2015; Derksen *et al.,* 2016). Yet, from 1988 to 2010, significant snow cover increases ($p < .01$) have been found during October across Eurasia, and these are posited to be the result of changing large-scale atmospheric patterns (Cohen *et al.,* 2012).

Total precipitation is expected to increase in the Arctic (Walsh *et al.,* 2008; AMAP, 2017) given that a warmer atmosphere has a higher holding capacity for water vapour, and this is supported by observations of increased poleward atmospheric moisture transport (Zhang *et al.,* 2012). To date, surface observations have largely shown a mix of increasing and decreasing precipitation trends, depending on season, location and analysis period (Hinzman *et al.,* 2005; Wendler and Shulski, 2009; McAfee *et al.,* 2013a; 2013b). However, observations of snow water equivalent from the GlobSnow v2.0 dataset (ESA, 2014) indicate significant ($p < .05$; two tailed t test) decreases of snowfall across North America for both February and April from 1980 to 2012; March also showed declines, but these have not quite reached the level of statistical significance (Jeong *et al.,* 2017).

Snowfall represents the dominant precipitation type at many locations in Alaska for several months of the year, and its water equivalent gets stored on the landscape rather than immediately running off. During the spring melt season—typically the driest period across Alaska (see Figure 6, Bieniek *et al.,* 2012)—the snowpack serves as the primary water source for soil recharge that is needed for plant life (Clilverd *et al.,* 2011), including uptake by trees in the boreal forest (Young-Robertson *et al.,* 2016). As the future climate is projected to warm, however, some of the precipitation that historically fell as snow is expected to fall as rain instead (McAfee *et al.,* 2013a; 2013b). One of the factors involved in this rain/snow partitioning is elevation, and it is anticipated that, while most locations will experience reduced snowfall, high elevations could see an increase in midwinter (Frei *et al.,* 2018).

Alterations to snow-related hydrological processes in Alaska could change the frequency and intensity of certain hazardous weather events. Rain-on-snow events, for example, produce a layer of ice on the surface that makes travel dangerous and inhibits foraging animals from accessing their winter food sources. Warming temperatures are expected to lead to an increased frequency of these events across the Arctic, including Alaska (Rennert *et al.,* 2009; Bieniek *et al.,* 2018). Unlike locations outside the Arctic—where temperatures often temporarily rise above freezing during winter—in mainland Alaska a layer of ice that forms on the surface can persist for months (Bieniek *et al.,* 2018). Warmer temperatures can also promote extreme snowfall, given the necessary thermodynamics. O'Gorman (2014) notes that extreme snowfall typically happens inside a specific temperature range. Heavy snowfall and a subsequent deep snowpack can lead to infrastructure failure (Strasser, 2008) and make it difficult for fauna (e.g., moose, caribou) to navigate the landscape (Dussault *et al.,* 2005).

Snow also helps to regulate the thermal and hydrologic properties of the soil that it covers. It is estimated that 38% of mainland Alaska contains near-surface permafrost (NSP; Pastick *et al.,* 2015), which is soil that is continually frozen throughout the year. The presence of snow cover acts to insulate the soil directly beneath it, keeping it warmer in the winter and making permafrost more vulnerable to thaw in the spring and summer. Alternatively, delayed spring melt keeps the surface closer to freezing and slows warming of the permafrost. When permafrost thaws, long-frozen organic compounds are able to decompose, releasing methane and carbon dioxide into the air, and amplifying the Arctic response to greenhouse warming (Walter Anthony *et al.,* 2016). In many areas, an active layer that exists above the permafrost is frozen for part of the year and thaws in the summer. Trends of near-surface permafrost temperature (i.e., 0–20 m beneath the surface) in northern Alaska indicate a warming of 0.5–2.0°C since the early 1980s (Brown and Romanovsky, 2008). When permafrost thaws, it causes subsidence of the land surface, which damages any built infrastructure on it (e.g., roads, buildings, pipelines).

Projections of 21st-century warming suggest that permafrost thaw will lead to the second highest costs associated with climate change in Alaska, behind only flooding (Melvin *et al.,* 2016). Using a multi-model ensemble from the CMIP5, Peng *et al*. (2018) found that active layer thicknesses across northern Alaska are projected to increase by 20 cm between 2071–2100 and 1971–2000. Overall, they found that soil temperatures at 1 m depth are projected to warm between 1 and 4°C (2080–2099 minus 1950–1969). Lawrence and Slater (2010) studied the relative impacts to NSP of changes in snow season length and snow depth, finding mixed results. Later snow onset in Alaska cooled the soil due to sub-freezing temperatures with minimal absorbed solar radiation, but an earlier melt yielded increasing soil temperatures. A shallower winter snowpack reduced the snow's insulating effect and contributed to cooling. A subsequent study by Lawrence *et al*. (2012) investigated how climate model biases of temperature and snow depth impact projections of NSP. Using an offline version of the land model from CCSM4, one that used observed meteorological data to initialize the permafrost state rather than using the warm and wet biased climate model, the magnitude of permafrost loss was 29% less by 2100.

Given the observed changes to important snow-related features in Alaska and the potential impacts that may result, this research investigates projections of snow season characteristics for Alaska using a set of dynamically downscaled climate model and reanalysis simulations from 1981 to 2100. The relatively high resolution of the downscaled simulations (20 km) represents an improvement on previous work that relied on coarse global climate models. Moreover, the dynamical forcing produces a full suite of daily meteorological variables, which is often not feasible for statistically downscaled datasets that rely on limited observational data as a basis for their empirical relationships. The primary targets of this assessment of recent and future changes of snow in Alaska are: (a) the anticipated change of the annual snowfall cycle according to elevation, (b) the resultant end-of-winter snow-water equivalent (SWE) as a function of elevation, (c) expected variations to snow onset and snowmelt dates and (d) expected changes in extreme snowfall events for population centres across Alaska.

2 | DATA AND METHODS

Regional dynamically downscaled climate model simulations are used to investigate projected snow season changes by 30-year periods (i.e., 2011–2040, 2041–2070 and 2071–2100), relative to a historical period from 1981 to 2010 across the Alaska domain (Figure 1). Specifically, the National Center for Atmospheric Research (NCAR) Community Climate System Model version 4 (CCSM4) and National Oceanic and Atmospheric Administration (NOAA) Geophysical Fluid Dynamics Laboratory Climate Model version 3 (GFDL-CM3; Donner *et al.,* 2011) are downscaled using the Weather Research and Forecasting Model (WRF; Skamarock *et al.,* 2008). The CCSM4 and GFDL-CM3 are members of the Coupled Model Intercomparison Project Phase 5 (CMIP5; Taylor *et al.,* 2012) with atmospheric model resolutions (latitude × longitude) of approximately 1° × 1.25° and 2° × 2.5°, respectively. Thus the downscaled data, which have a spatial resolution of 20-km, are more than four times finer than the original forcing data. The future simulations are based on representative concentration pathway 8.5 (RCP8.5; Riahi *et al.,* 2011), which best tracks the current trajectory of greenhouse gas emissions (Peters *et al.,* 2013).

Regional orography, represented by the downscaling procedure, is displayed in Figure 1. Superimposed on this map are 21 stations across Alaska that have a minimum of 95%

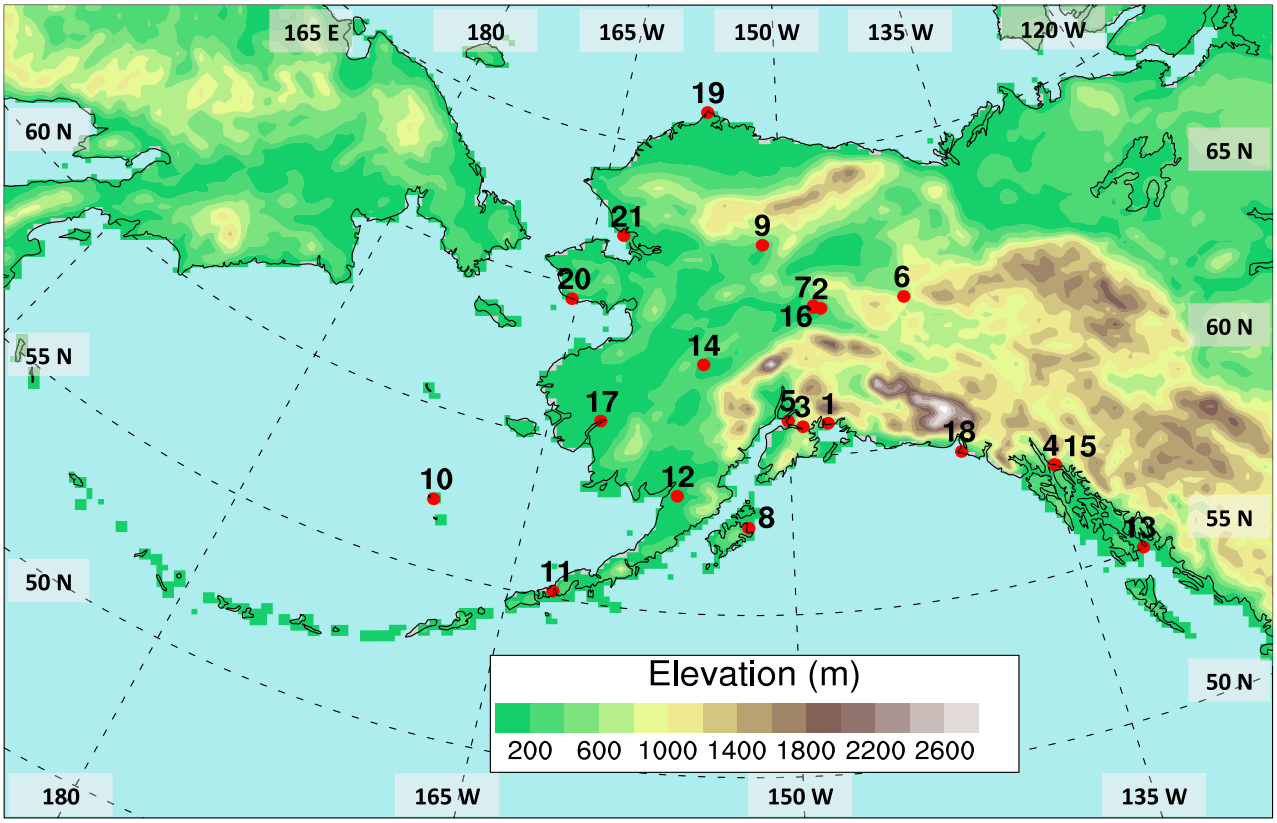

FIGURE 1 Distribution of stations, superimposed on regional orography, with ≥95% daily coverage (1981–2010) of precipitation, snowfall and snow depth. A description of the numbered stations is located in Table 1

daily coverage of precipitation, snowfall and snow depth during the historical period (1981–2010). These data are available from the Global Historical Climatology Network Daily (GHCN-D) database (Menne *et al.,* 2012; https://www.ncdc.noaa.gov/ghcn-daily-references). Precipitation at these stations is measured with a rain gauge and snowfall is recorded with a snow measurement board. Table 1 lists average cold-season (i.e., all months excluding May–September) precipitation and snowfall for all 21 stations used in this study. The stations all have relatively low elevation in common; the highest location, Eagle, is at 259 m, and 15 of the stations are situated less than 100 m above sea level. They have widely varying cold season precipitation and snowfall amounts, however. Yakutat receives 2,475 mm of precipitation, on average, each cold season, whereas Utqiaġvik typically records 33 mm. Utqiaġvik also receives the least snowfall (74 cm), and Alyeska has the highest, averaging 547 cm. Each of the eight stations that show significantly increasing snowfall trends are close to the coast.

Given the paucity of meteorological observations with adequate temporal coverage for climate studies across Alaska, especially for higher elevations, reanalysis data can be used instead as a proxy source of gridded observations. This study utilizes a dynamically downscaled simulation of the ERA-Interim reanalysis (Dee *et al.,* 2011) that covers the historical period (1981–2010), and uses the same WRF parameterizations as was done with simulations driven by CCSM4 and GFDL-CM3. Among reanalysis models, the ERA-Interim frequently displays the lowest temperature and precipitation bias when compared to observations in Alaska (Lader *et al.,* 2016) and the broader Arctic (Lindsay *et al.,* 2014).

The downscaling simulations are initialized every 48 hr, and forecasts are produced to 54 hr with every first 6 hr discarded to allow for spin-up. Spectral nudging is used to constrain the downscaled products to the original ERA-Interim (Bieniek *et al.,* 2016). Relative to the coarser reanalysis, the downscaled reanalysis data have been shown to provide a closer representation of daily temperature and precipitation

TABLE 1 Station information and annual cold season (i.e., all months excluding May–September) mean ($\bar{x}$), standard deviation (s) and trend of precipitation (PCPT; mm) and snowfall (SNOW; cm) from 1981 to 2010. Trend significance ($p < .05$; Student's t test) is shown in bold

					PCPT			SNOW		
Num.	**Station name**	**Lat. (°N)**	**Lon. (°W)**	**Elev. (m)**	$\bar{x}$	s	**mm/decade**	$\bar{x}$	s	**cm/decade**
1	Cannery Creek	61.0	147.5	26	1,739	319	−38	353	110	19
2	North Pole	64.8	147.3	145	113	80	−18	124	54	−14
3	Alyeska	61.0	149.1	83	1,251	309	36	547	168	**106**
4	Auke Bay	58.4	134.7	13	849	194	−25	201	102	16
5	Anchorage	61.2	150.0	37	170	40	−5	190	53	**22**
6	Eagle	64.8	141.2	259	102	23	4	152	38	−5
7	College	64.9	147.9	182	107	41	−12	158	68	−25
8	Kodiak	57.8	152.5	24	1,266	257	38	190	80	26
9	Bettles	66.9	151.5	196	145	52	20	221	70	7
10	St. Paul Island	57.2	170.2	11	343	71	−8	147	68	**34**
11	Cold Bay	55.2	162.7	24	646	203	60	184	65	5
12	King Salmon	58.7	156.7	20	211	57	−8	124	47	11
13	Annette	55.0	131.6	33	1,771	257	29	84	52	**24**
14	McGrath	63.0	155.6	102	196	67	−11	241	82	−19
15	Juneau	58.4	134.6	5	928	228	75	220	113	28
16	Fairbanks	64.8	147.9	132	95	34	**−14**	157	64	−24
17	Bethel	60.8	161.8	31	186	54	17	152	53	**36**
18	Yakutat	59.5	139.7	10	2,475	688	**−305**	399	157	12
19	Utqiaġvik	71.3	156.8	9	33	13	**7**	74	35	**34**
20	Nome	64.5	165.4	4	182	46	−2	187	55	**33**
21	Kotzebue	66.9	162.6	9	123	42	13	152	53	**35**

when compared to observations in Alaska (Bieniek *et al.,* 2016; Lader *et al.,* 2017).

3 | RESULTS

3.1 | Validation

The spatial distributions of accumulated snowfall (ACSNOW) from the downscaled ERA-Interim, after summation by month and averaging over the historical period, are displayed in Figure 2. The ACSNOW variable is the daily accumulation of snowfall in terms of its water equivalent. Mainland Alaska experiences its greatest ACSNOW during October (Figure 2b) and November (Figure 2c). Thereafter, the winter sea ice develops, which acts to reduce local surface evaporation (Bintanja and Selten, 2014), and monthly ACSNOW decreases. Much of southern Alaska displays its largest ACSNOW amounts during December (Figure 2d) and January (Figure 2e). Mountainous locations, particularly the high peaks of the Alaska Range, receive accumulating ACSNOW during all months, albeit considerably less in the summer.

Snowfall is particularly difficult to measure; in fact, eight of the 21 stations in Table 1 display opposing trends of observed precipitation and snowfall during the historical period. Given that a large portion of winter precipitation falls as snow at these stations, it should follow that the trends are of the same sign. It is possible that there is a physical basis for this discrepancy (e.g., local changes to how precipitation is partitioned between rain and snow), or this could result from differences in the measurement method. Snowfall at these stations is measured with a snow measurement board and liquid precipitation with a gauge. Previous studies have also documented the challenges (e.g., wind-caused undercatch, various shielding methods) associated with in situ snowfall measurements in precipitation gauges (Yang *et al.,* 1998a; 1998b; Adam and Lettenmaier, 2003; Kotlarski *et al.,* 2012).

Correlations between historically observed precipitation at Utqiaġvik, Fairbanks and Nome and the ACSNOW variable from their coincident downscaled ERA-Interim grid cells are statistically significant for each of the core winter months (i.e., December through March) ($p < .05$, Student's t test; Figure 3). It is assumed that snow was the predominant precipitation type at these stations because the average temperature from 1981 to 2010 during these months at Utqiaġvik, Nome and Fairbanks was −24.6, −17.8 and − 13.3°C, respectively (NOAA, 2018). From December through March, the monthly linear regression between observed precipitation and ERA-Interim ACSNOW provides slope values (i.e., change in ACSNOW per change in observed precipitation) that range between 0.94 and 1.09 for Fairbanks, 1.06 and 1.37 for Nome and 1.31 and 2.83 for Utqiaġvik. This indicates that the largest overestimation of ACSNOW from the reanalysis occurs at Utqiaġvik. The overestimation of ACSNOW by the forecast model makes sense given that wind-induced undercatch of snowfall by the precipitation measurement is a significant problem for sites in Alaska (Yang *et al.,* 1998a; 1998b). Thus, these relationships between observed station precipitation and ACSNOW from the coincident ERA-Interim grid cell, at widely disparate locations, provide a measure of confidence that the downscaled ACSNOW variable reasonably captures snowfall across northern Alaska. Outside of the core winter months and for more southerly locations, where precipitation is more rainfall dominant, the correlations between observed precipitation and downscaled ACSNOW are lower. A second limitation to this relationship is that these stations are all at low elevation; the "observed precipitation/modeled ACSNOW" relationship might not hold at higher elevations.

Future projections in Section 3 are frequently discussed in reference to the downscaled CCSM4 and GFDL-CM3 historical periods (1981–2010). The historical CCSM4 bias of ACSNOW relative to the downscaled ERA-Interim ACSNOW from 1981–2010 can generally be described as positive for most of western and central Alaska; this is especially true for the western Brooks Range (Figure 4). The most substantial negative ACSNOW bias from CCSM4 occurs in southeast Alaska in January, and, to a lesser extent, across the eastern Interior over the September through October period (Figure 4). The historical GFDL-CM3 ACSNOW biases are frequently smaller than for CCSM4. The GFDL-CM3 has a positive ACSNOW bias across the Brooks Range and North Slope, small and mixed biases for southwestern and Interior Alaska, and a negative ACSNOW bias for southeast Alaska that is most pronounced during January (Figure 5). The historical CCSM4 ACSNOW amounts, expressed as percentages of the total statewide ERA-Interim ACSNOW, range from 124.8% in December to 158.4% in November. The monthly statewide ACSNOW amounts from GFDL-CM3 range from 90.7% of the ERA-Interim amount in February to 168.1% in September. Except for the month of September, GFDL-CM3 has the lowest historical ACSNOW bias relative to ERA-Interim.

3.2 | Elevation dependency of projected ACSNOW

The statewide annual cycle of monthly ACSNOW for both climate models, produced by the summation of daily values that are averaged by 30-year periods, is shown in Figure 6. These climatologies represent the historical period (1981–2010; thick black lines) and three future periods (2011–2040; 2041–2070; 2071–2100) and are based on the

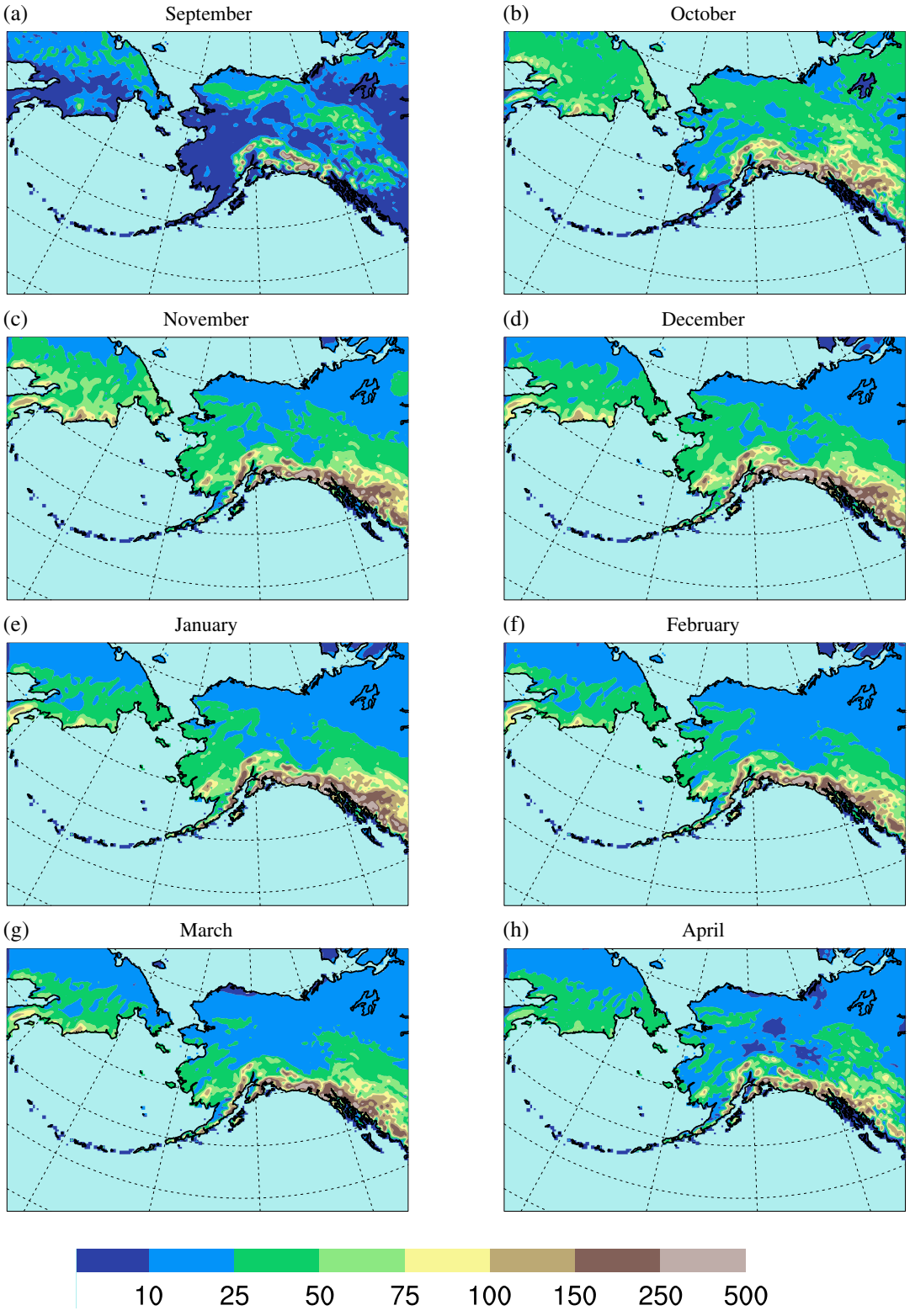

FIGURE 2 Average total monthly water equivalent of accumulated snow (ACSNOW; mm) from downscaled ERA-Interim (1981–2010)

RCP8.5 emissions scenario for CCSM4 (Figure 6, left) and GFDL-CM3 (Figure 6, right). The climatologies are further divided into two elevation bins: low grid cells (0–1,000 m; Figure 6a) and high grid cells (1,000–2,000 m Figure 6b). Only 30 of the 3,691 land grid cells used in this study are above 2,000 m in the downscaled model topography, so

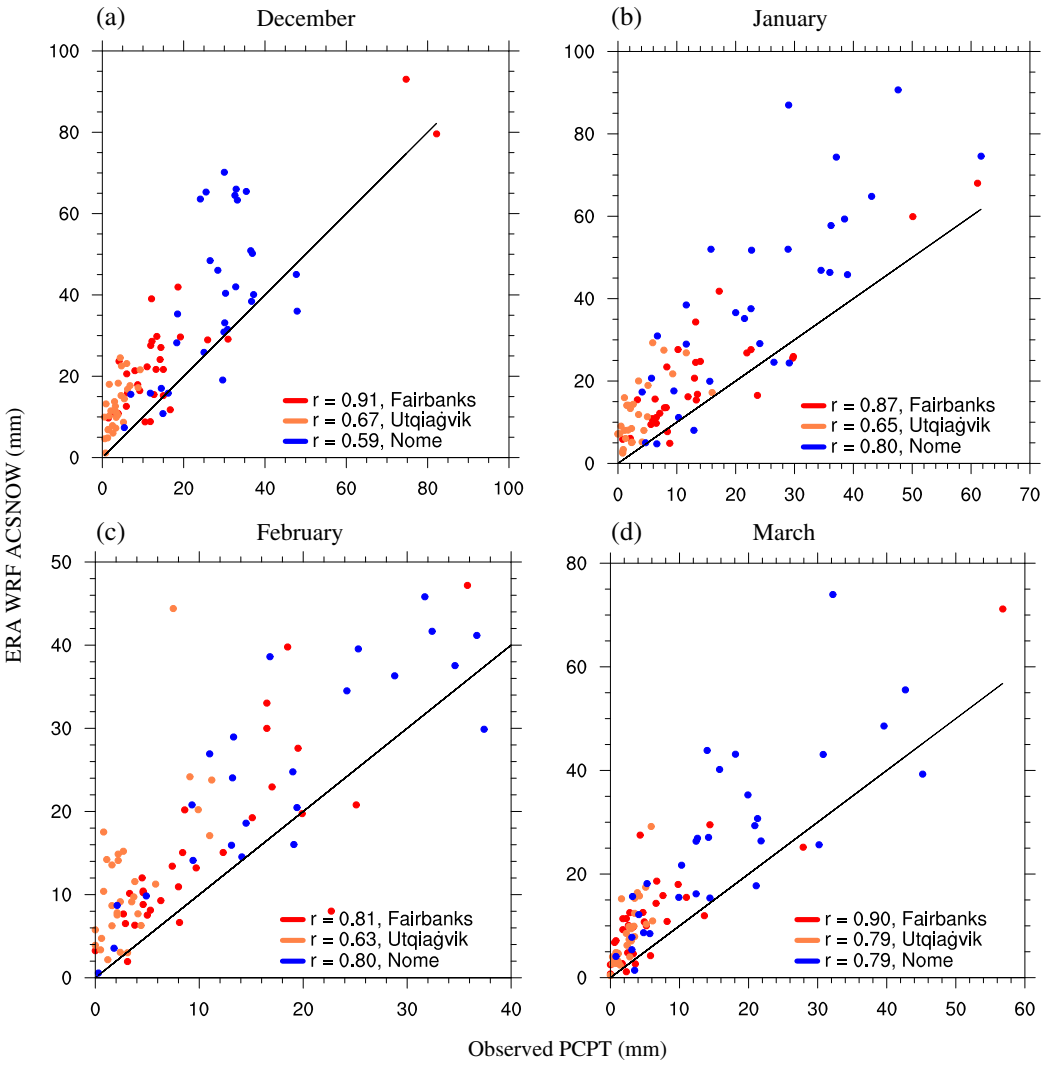

FIGURE 3 Scatterplots between total monthly observed precipitation (PCPT; mm) at three stations: Fairbanks International Airport (red), Wiley Post-Will Rogers Memorial Airport (Utqiaġvik (Barrow); green), and Nome Airport (blue) and downscaled ERA-Interim water equivalent of accumulated snow (ACSNOW; mm) from 1981 to 2010. Correlation coefficient (r) is provided with the legend and all values are statistically significant ($p < .05$; Student's t test)

elevations above 2,000 m were left out of the analysis. The historical ERA-Interim climatologies for the two elevation bins are shown with thick grey lines in Figure 6. When comparing the historical ERA-Interim with each of the climate models' historical climatologies, it is evident that the GFDL-CM3 has the best agreement. The historical CCSM4 has a positive bias for both elevation bins that is most distinct from October through April.

At low elevations (Figure 6a), CCSM4 and GFDL-CM3 show decreased ACSNOW in nearly every month with the advance of each 30-year period. CCSM4 produces more ACSNOW than GFDL-CM3 during all periods; however, the magnitude of the discrepancy between the two models is lowest at the end of the century. The greatest monthly ACSNOW depicted by CCSM4 during the historical period is 70.1 mm for January, but for GFDL-CM3 the highest value occurs in December (47.1 mm). For the late-century (2071–2100), the peak monthly value for CCSM4 is 50.8 mm, and for GFDL-CM3 it is 39.7 mm, both in December. When comparing the late-century with the historical period, the annual ACSNOW reductions at low elevations, by percentage, are 41.3 and 40.6% for CCSM4 and GFDL-CM3, respectively.

At high elevations (Figure 6b), projected changes in the annual ACSNOW cycle are dependent on the month. From May–October, both models show reduced amounts, with the summer months depicting nearly no ACSNOW by the late century. During the months with the least incoming solar radiation (i.e., November, December and January), GFDL-CM3 shows increased ACSNOW during the late-century; likewise, CCSM4 displays increases in December. The increased winter ACSNOW and decreased warm season

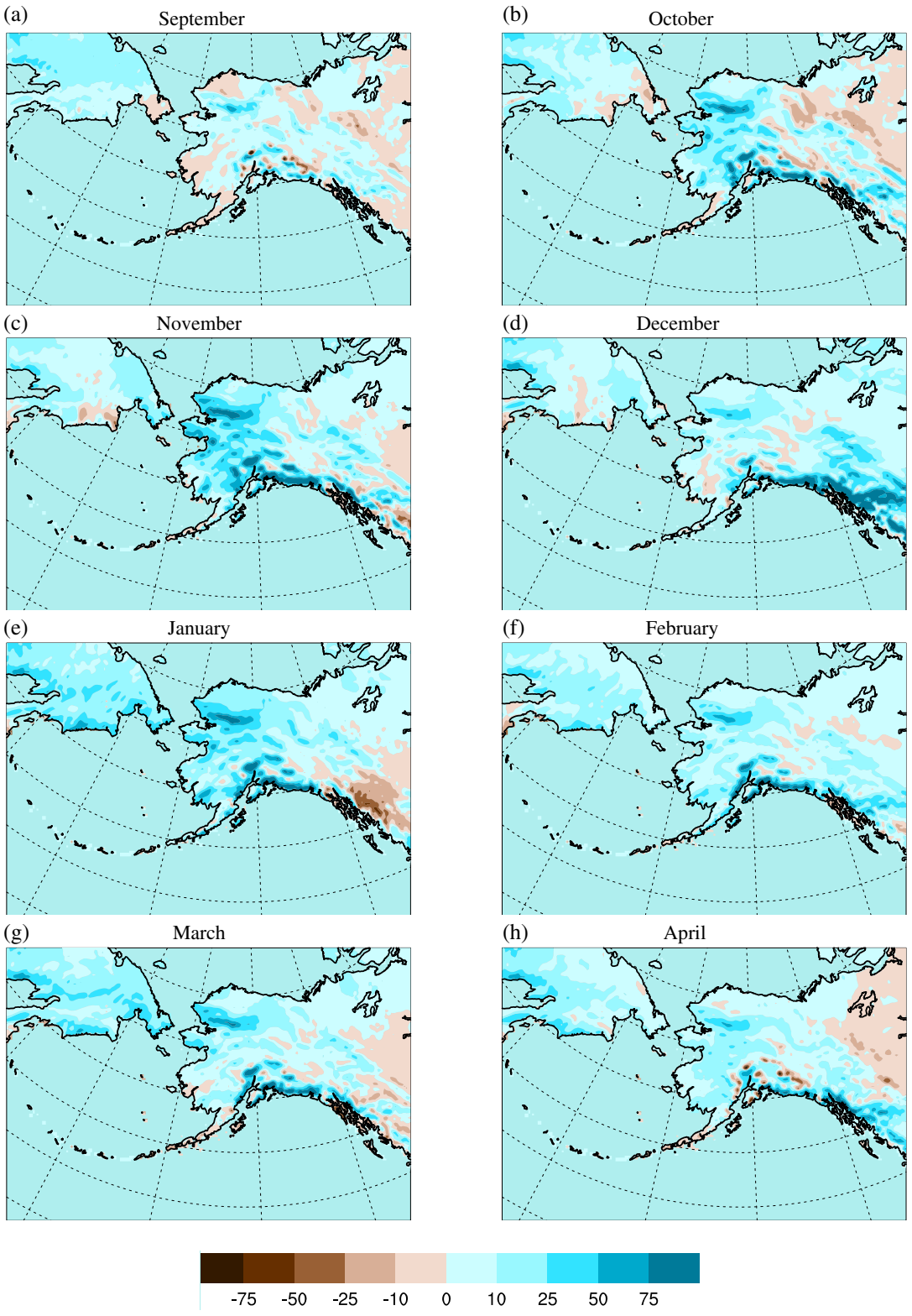

FIGURE 4 CCSM4 bias (CCSM4 1981–2010 minus ERA-Interim 1981–2010) of average total monthly water equivalent of accumulated snow (ACSNOW; mm)

ACSNOW combine to overall annual high-elevation reductions of 13.5 and 14.2% for CCSM4 and GFDL-CM3, respectively. The percentage reductions are much smaller than at lower elevations. Similar to the low elevation grid cells, CCSM4 generally produces more ACSNOW at high elevations than does the GFDL-CM3.

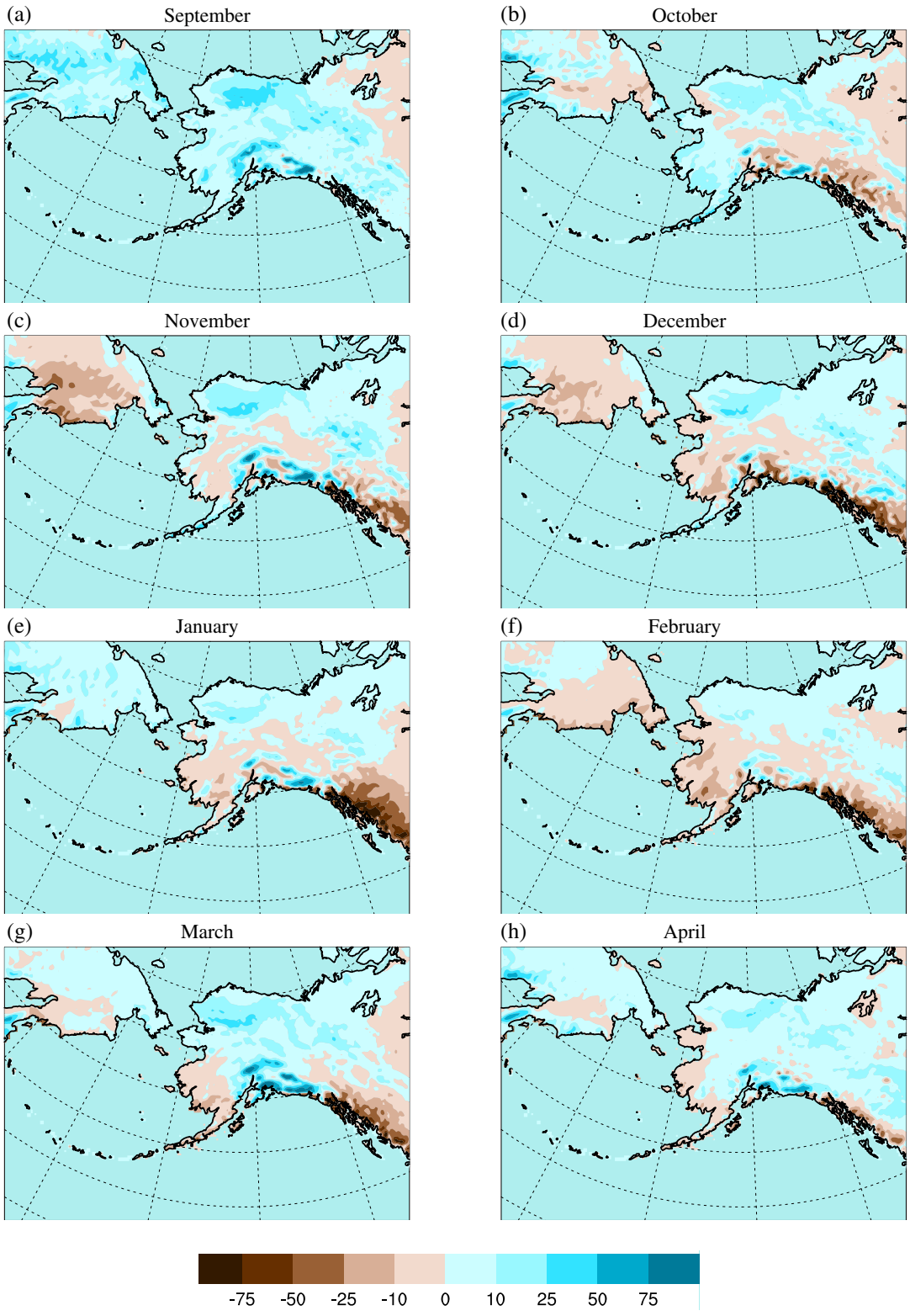

FIGURE 5 GFDL-CM3 bias (GFDL-CM3 1981–2010 minus ERA-Interim 1981–2010) of average total monthly water equivalent of accumulated snow (ACSNOW; mm)

The April 1 (e.g., end-of-winter) SWE, binned into 100 m elevation intervals and averaged over the same 30-year periods as before, is shown for CCSM4 (Figure 7a) and GFDL-CM3 (Figure 7b). The historical ERA-Interim is shown with thick grey lines. The historical CCSM4 (Figure 7a; thick black line) tracks closely with the ERA-

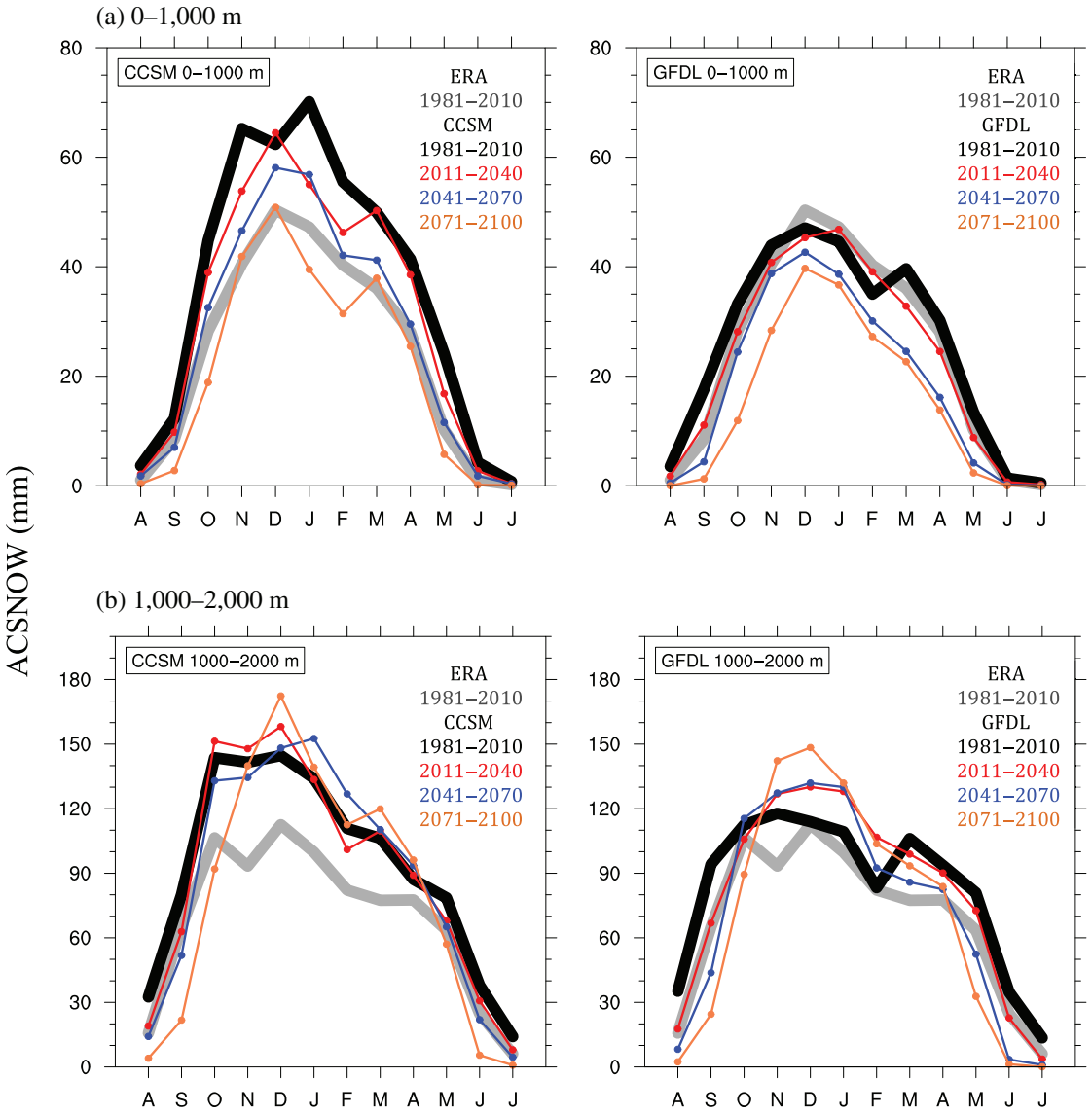

FIGURE 6 Monthly averaged water equivalent of accumulated snow (ACSNOW; mm) for elevations (a) 0–1,000 m and (b) 1,000–2000 m. These climatologies represent the downscaled CCSM4 (left) and GFDL-CM3 (right) for 30-year periods across Alaska. These include: 1981–2010 (thick black), 2011–2040 (red), 2041–2070 (blue) and 2071–2100 (brown). The thick grey lines show the downscaled ERA-Interim climatologies from 1981 to 2010

Interim for all the elevation bins up to 1,000 m; the GFDL-CM3 shows good agreement up to 500 m, but has a positive bias from 500 to 1,000 m (Figure 7b). For the same reason that the ACSNOW analysis was restricted to elevations at and below 2,000 m (i.e., limited number of grid cells), the April 1 SWE analysis, which uses a finer elevation bin resolution of 100 m, is restricted to the lowest 1,000 m. While the two climate models exhibit similar April 1 SWE up to 500 m elevations, the GFDL-CM3 depicts a thicker snowpack that is 22.5 mm deeper than CCSM4 in the 900–1,000 m bin. The apparent contradiction between GFDL-CM3 having higher April 1 SWE values above 500 m despite CCSM4 having larger monthly ACSNOW biases (Figure 6) could be an artefact of the binning process or be related to model physics, such that the CCSM4 melts more snow during the winter. With each 30-year advance, April 1 SWE is projected to decrease and the greatest reductions, by percentage, occur at the lowest elevations. At the lowest interval (i.e., 0–100 m), CCSM4 shows a 62.8% decrease from 96.5 to 35.9 mm by the late century. For GFDL-CM3, these values are 85.5 mm to 16.0 mm, representing an 81.3% decrease. GFDL-CM3 shows larger reductions at every level, such that despite having greater SWE during the historical period, it displays lower values at every elevation by the late century.

One reason for these SWE reductions is that the ratio of snow to total precipitation is projected to decrease. During the historical period, snow represented 47.8 and 41.5% of

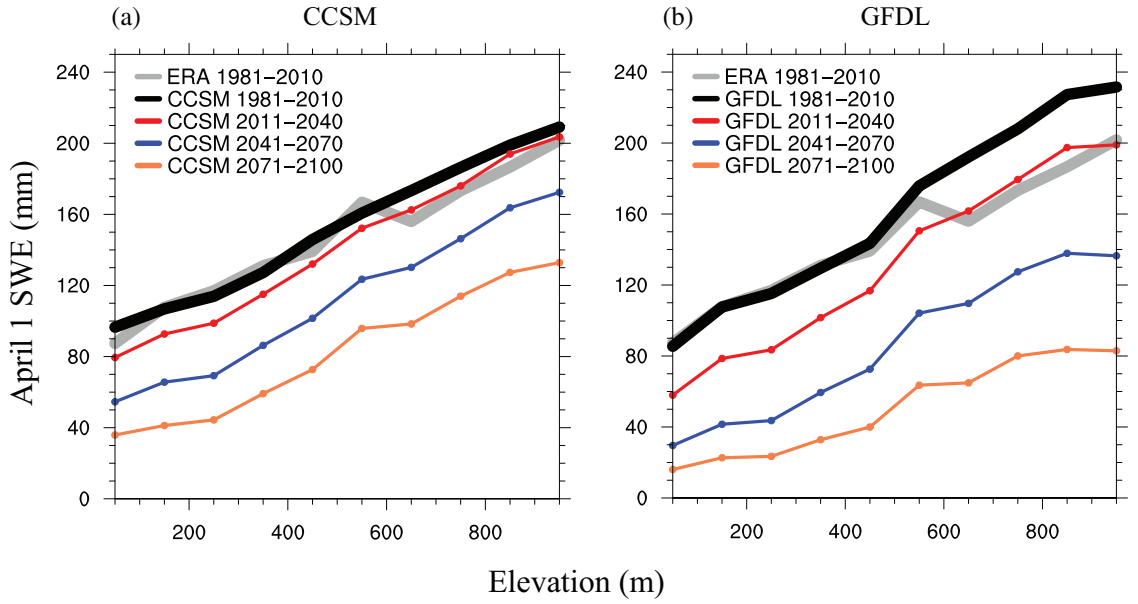

FIGURE 7 April 1 snow-water equivalent (SWE; mm) for (a) CCSM4 and (b) GFDL-CM3. Downscaled grid cells have been binned in 100-m elevation intervals and averaged for 30-year periods across Alaska. These include: 1981–2010 (thick black), 2011–2040 (red), 2041–2070 (blue) and 2071–2100 (brown). The thick grey lines show the downscaled ERA-Interim climatologies from 1981 to 2010

the total precipitation that fell in Alaska from September–November (SON) for CCSM4, and GFDL-CM3, respectively. For the late-century period, these values are projected to drop to 24.8 and 16.7%. For meteorological winter (DJF), 80.7% (CCSM4) and 75.9% (GFDL-CM3) historically fell as snow; however, these percentages drop to 51.4, and 46.8% by the late-century, respectively. Thus, considerably more rainfall is anticipated during the cold season.

3.3 | Changes to snow season length

Each cold season, mainland Alaska has historically experienced a continuous period with snow cover. The snowmelt date, defined as when SWE is less than or equal to 2.0 mm for the first time in a given year (Sun *et al.,* 2016), exhibits a wide range across Alaska according to the ERA-Interim (Figure 8a). Many mountainous and northern locations do not melt out until late-May or June. Interior areas generally lose their snowpack during late April or early May, while low elevations in southern Alaska melt out during March and April. Some coastal areas in the Aleutian Islands and southeast Alaska do not have continuous snow cover during the winter. Both the CCSM4 (Figure 8a, middle) and GFDL-CM3 (Figure 8a bottom) show later snowmelt dates for areas of the Brooks Range, North Slope, eastern Interior and southeast Alaska; they both also show earlier snowmelt dates for southwest Alaska. These biases are generally within 1–2 weeks of the climatological ERA-Interim date; however, the climate models indicate later snowmelt dates of 1–2 months across the higher terrain of southeastern Alaska. However, there is higher uncertainty in these glacial regions of southeast Alaska. Note that there is an area in Figure 8 that has been masked out. This is because many alpine grid cells in the coarse ERA-Interim are parameterized to have 10,000 mm of SWE, an unrealistically high value (Drusch *et al.,* 2004). This, in turn, produces unrealistic SWE values in the downscaled simulation. An artefact of this masking process is visible in Figure 7 for the April 1 ERA-Interim SWE. A disproportionate number of the adjacent high-SWE grid cells in southern Alaska that were not masked out are between 500 and 600 m elevation, which results in the step-like feature from 500 to 700 m.

The snow onset date, when SWE is continuously greater than or equal to 2.0 mm, historically occurs typically during late September for the North Slope, October for the Interior and November for south and southwest Alaska (Figure 8b). The historical CCSM4 bias of snow onset date (Figure 8b, middle) shows a later onset for southwest Alaska and the western Interior, generally of 1–2 weeks; GFDL-CM3 (Figure 8b, bottom) shows comparable spatial patterns with slightly larger positive biases for southwest Alaska and an earlier snow onset across northeast Alaska. Note that the high-elevation grid cells in southeast Alaska show substantial biases, but these may be due more to parameterization issues and uncertainty than model bias. An attempt was made to use the GlobSnow-v2 SWE dataset (ESA, 2014) as historical gridded "observations"; however, after interpolation and re-gridding to the WRF grid, it was found that this

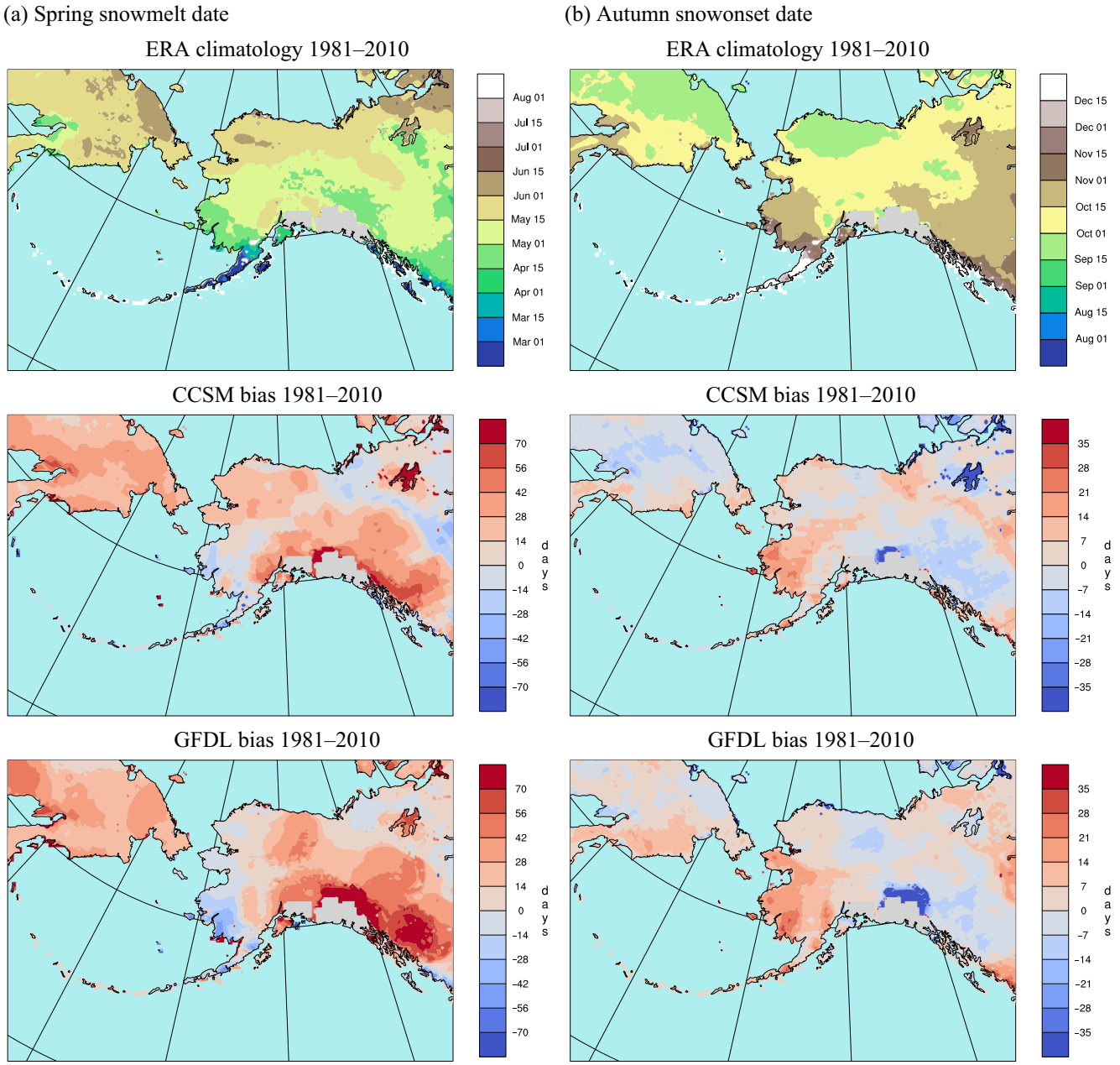

FIGURE 8 Climatological (1981–2010) (a) spring snowmelt date and (b) autumn snow onset date for downscaled ERA-Interim (top), and climate model bias from CCSM4 (middle) and GFDL-CM3 (bottom). Red (blue) shading indicates that the climate model has a later (earlier) date than ERA-Interim. A portion of southern Alaska (grey) has been masked out due to an unrealistically high SWE parameterization in the original ERA-Interim

new product lacked topographic detail and was not suitable for comparison with a dynamically downscaled product that resolved Alaska's topography with finer resolution. Moreover, the future projections utilize both the ACSNOW and SWE variables, and the former is compared to the ERA-Interim, thus it is for consistency that both of these snow season variables are presented and discussed in relation to the ERA-Interim.

Projections of snowmelt indicate earlier dates that range from approximately 1 month across high terrain and Interior Alaska, to complete loss of continuous winter snowpack in southwest Alaska by the second half of the century (Figure 9). For the nearest downscaled CCSM4 grid cell to Utqiaġvik, the historical snowmelt date is June 15, and it is projected to advance to May 27 during 2071–2100; for GFDL-CM3 these dates are June 22 and April 16. The historical observed mean spring snowmelt date from the GHCN-D station data for Utqiaġvik is May 27. The Nome grid cell displays much larger changes, however. The historical values for CCSM4 and GFDL-CM3 are May 24 and

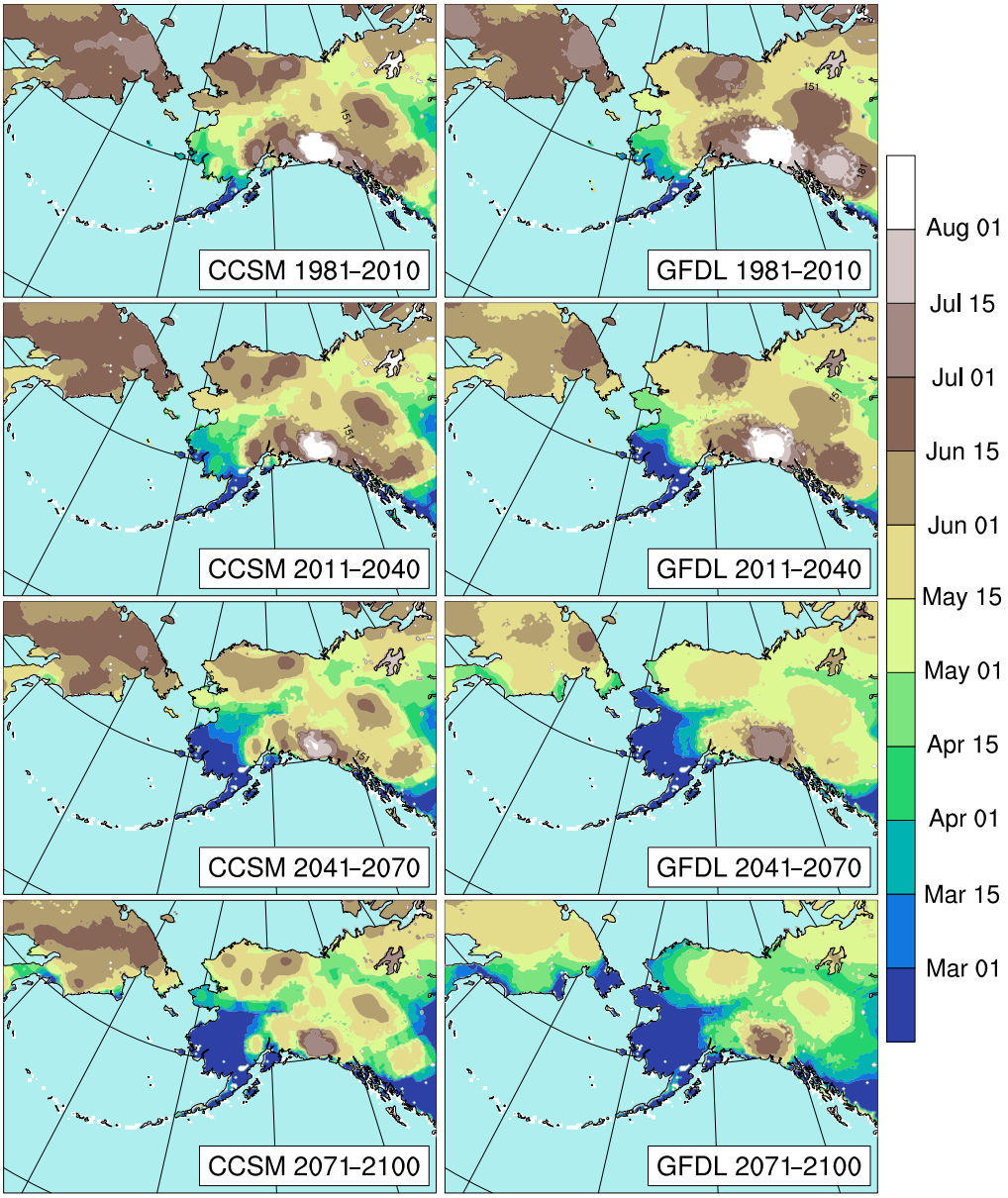

FIGURE 9 Snowmelt date (SWE ≤ 2 mm) averaged for downscaled CCSM4 (left) and GFDL-CM3 (right) over the indicated 30-year periods across Alaska

April 19, and these advance to February 7 and January 26, respectively. The historical GHCN-D date is May 9. This dramatic change is possibly due to Nome's closer proximity to the seasonal sea-ice edge. The Bering Sea is projected to have more open water months by the end of this century (Wang and Overland, 2015), which means that the trajectory of incoming cyclones would cross more open water as opposed to ice, bringing warmer air and rainfall. Such early dates indicate an effective end to the presence of continuous winter snowpack at Nome. The discrepancies of snowmelt date between the nearest downscaled grid cells and the GHCN-D station observations possibly arise from model deficiencies and the spatial-scale mismatch between the gridded data, which represent areal averages, and point observations from coastal locations, which will generally be warmer than the averages for grid cells containing some land at elevation.

Snow onset dates from the historical CCSM4 (Figure 10, top left) and historical GFDL-CM3 (Figure 10, top right) show comparable spatial patterns. GFDL-CM3 shows a more delayed snow onset in the future periods, but both models indicate a later start to the snow season. The nearest downscaled CCSM4 grid cell to Fairbanks shows a historical snow onset of October 20 compared to a late-century onset of November 17. For GFDL-CM3 the average onset date shifts from October 17 to December 4. The historical observed snow onset date from the GHCN-D station data for Fairbanks is October 16. Along the

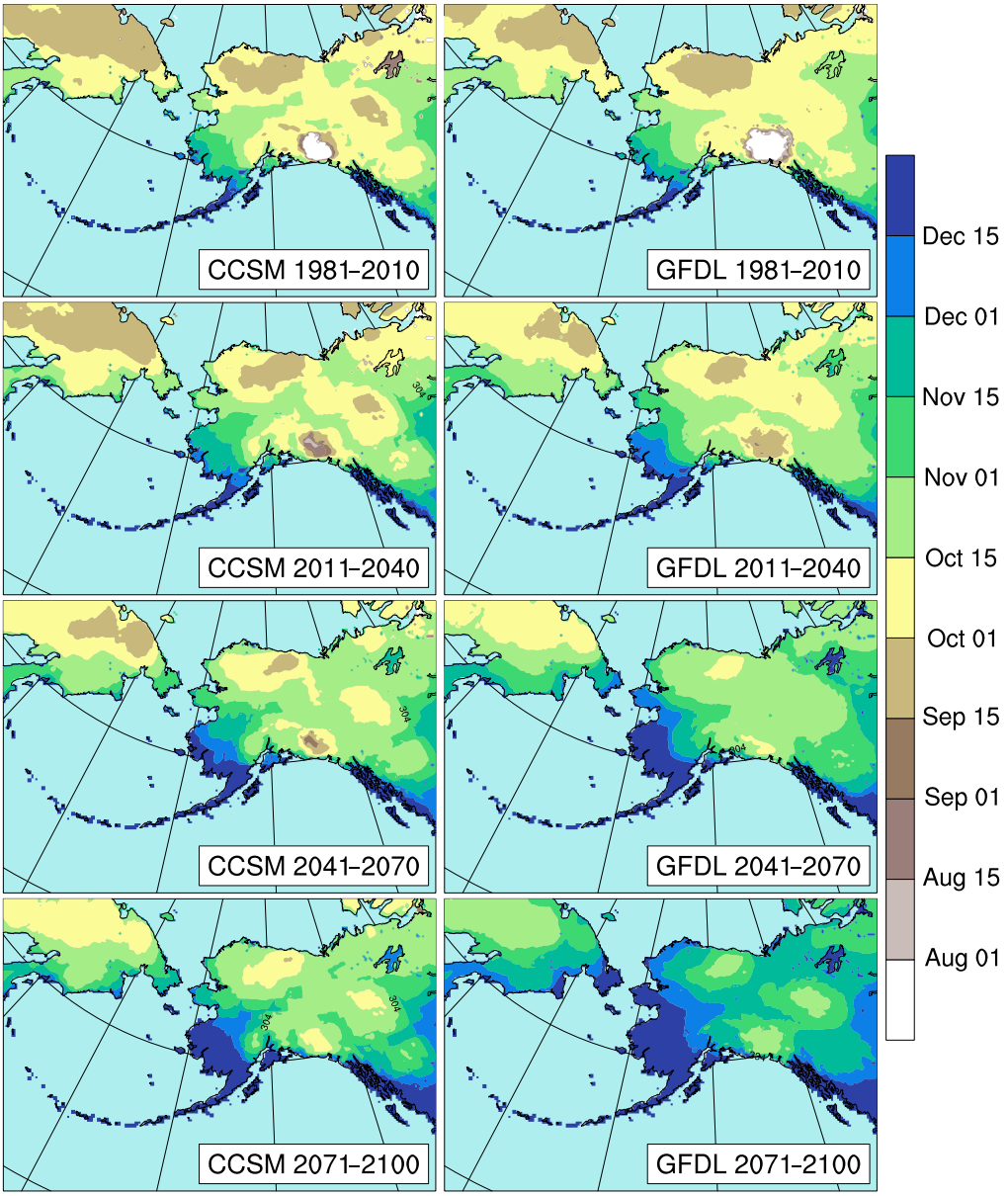

FIGURE 10 Snow onset date (SWE continuously ≥ 2 mm) averaged for downscaled CCSM4 (left) and GFDL-CM3 (right) over the indicated 30-year periods across Alaska

Arctic coast at Utqiaġvik, where the historical GHCN-D snow onset date is September 30, CCSM4 shows a change from October 8 to November 11, and GFDL-CM3 indicates a change from October 3 to December 14. The latter coincides with the absence of sea ice in the Chukchi and Beaufort Seas from 2071 to 2100 (see Figure 10, Lader *et al.,* 2017), which would support a maritime climate at Utqiaġvik even during winter.

3.4 | Projections of extreme ACSNOW

The annual maximum 2-day ACSNOW for the nearest downscaled grid cells to Anchorage, Utqiaġvik, Fairbanks and Nome (Figure 11a–d) show different responses that depend on location and time period. The total ACSNOW amount for two consecutive days is used, rather than a single day, to account for events that begin 1 day and continue into the next. At Anchorage, the median annual maximum ACSNOW reduces from 16.0 mm (CCSM4) and 14.1 mm (GFDL-CM3) during the historical period to 10.3 mm (CCSM4) and 7.8 mm (GFDL-CM3) for the late century. There is also a tendency for the absolute highest totals at Anchorage (upper ends of whiskers in Figure 11a) to occur during the historical and early-century periods. For Utqiaġvik and Fairbanks, a trend is not evident. When comparing the historical and late-century periods, CCSM4 indicates a slight decrease in the median annual maximum

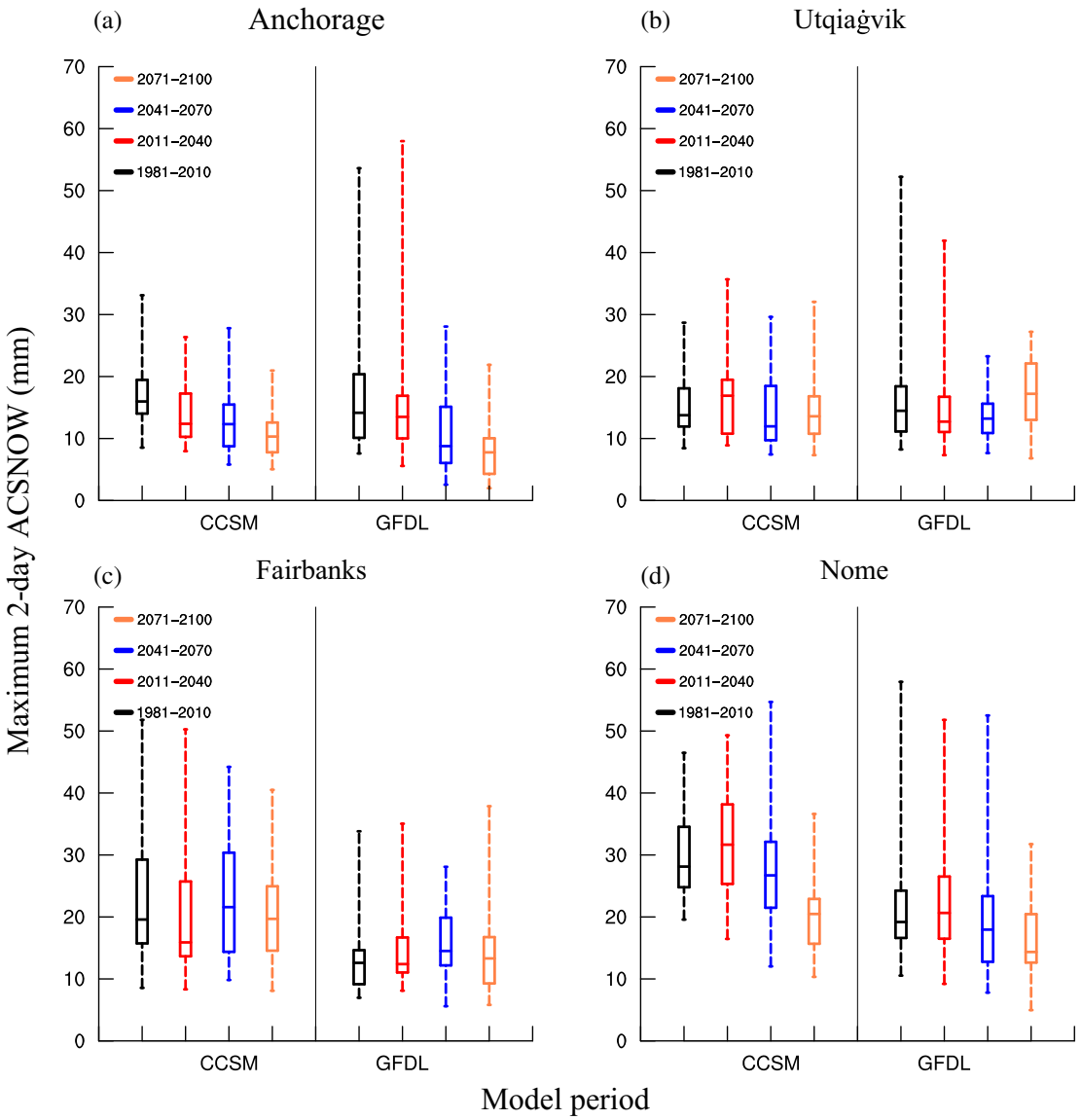

FIGURE 11 Boxplots of annual 2-day maxima of water equivalent of accumulated snow (ACSNOW; mm) for the nearest downscaled grid cells to (a) Anchorage, (b) Utqiaġvik (Barrow), (c) Fairbanks and (d) Nome. Boxes represent the median and interquartile range, and whiskers show the extremes for both CCSM4 and GFDL-CM3 for 1981–2010 (black), 2011–2040 (red), 2041–2070 (blue) and 2071–2100 (brown)

ACSNOW amount, but GFDL-CM3 shows an increase. Nome is similar to Anchorage in that the median annual maximum ACSNOW amount is reduced from 28.1 to 20.5 mm according to CCSM4 and from 19.2 to 14.3 mm for GFDL-CM3. The highest amounts at Nome (e.g., top 10) all occur in the earlier periods and by the late century there are many annual maximum ACSNOW amounts in the 5–15 mm range.

4 | DISCUSSION

A comparison of the projected annual cycle of ACSNOW with end-of-winter (i.e., April 1) SWE highlights the competing effects at work in future changes of snow over Alaska. For locations above 1,000 m, CCSM4 shows the highest December ACSNOW occurring in the late-century period, and GFDL-CM3 shows this for the 3-month period from November to January (Figure 6b). Below 1,000 m, ACSNOW is projected to decrease in every month and end-of-winter SWE is projected to decline for all elevations with the advance of each period (Figure 7). These latter results are similar to Schmucki *et al*. (2014), who looked at 21st-century projections of mean SWE for 11 stations in Switzerland with elevations ranging between 430 and 2540 m above sea level. The SWE reduction in Alaska cannot be fully explained by lower monthly ACSNOW in the late summer

and autumn. The 8-month ACSNOW sum below 1,000 m, beginning in August and ending in March, is only 32–39% lower in the late-century period than in the historical, depending on the model. However, reductions of SWE during this 8-month period average between 36–63% and 64–81% for CCSM4 and GFDL-CM3, respectively. The implication here is that considerable snowfall is projected to melt and runoff after it falls, which is consistent with results across the European mountain landscape (Beniston *et al.,* 2018) and locally in Alaska (Littell *et al.,* 2018).

Snow-season length, defined here as the continuous period with a minimum of 2.0 mm of SWE on the ground, shows unambiguous declines, but the rate of decrease depends on location and time period. The greatest changes are projected for the last two 30-year periods, corresponding to when the changes in projected radiative forcing from the RCPs diverge (Kunreuther *et al.,* 2014), thus suggesting that current decision-making can meaningfully impact the future snow season characteristics. For the Swiss Alps, Marty *et al.* (2017) found that the emissions scenario used had little effect on snow cover changes through mid-century; however, following an intervention scenario that limited warming to 2°C, drastically reduced changes thereafter.

Location-specific changes to snow season timing indicate a stronger tendency for earlier snowmelt than for later snow onset (Klein *et al.,* 2016). This is true for the nearest downscaled grid cell to Anchorage, Fairbanks and Nome for both models. Utqiaġvik shows a larger change to later snow onset than for earlier snowmelt. The projected rate of decline of snow-season length over the full period is generally higher than recently observed. Liston and Hiemstra (2011) noted a rate of −2.6% days/decade from 1979 to 2009 across the Arctic, but the rates found here are generally 2–5 times higher. Some of these differences likely relate to the spatial variability of change. Utqiaġvik, for example, has shown a trend for an earlier snowmelt date of 2.86 days/decade and a later onset date of 4.6 days/decade from 1975 to 2016 (Cox *et al.,* 2017), which taken together, suggests approximately a 1 week reduction in snow season length per decade.

Projected changes to ACSNOW extremes described in Figure 11 are consistent with previous studies that examined a large set of CMIP5 models across the Northern Hemisphere (Krasting *et al.,* 2013; Danco *et al.,* 2016). That is, despite a decrease in total annual snowfall for most locations, many sites are expected to continue to see high daily snowfall amounts. This is particularly true for more northerly, continental or high-elevation locations and for the core winter months. The four locations chosen in this study exhibit these patterns. Anchorage (Figure 11a) has a maritime climate and shows late-century decreases in the average annual 2-day maximum ACSNOW amount of 36% (CCSM4) and 53% (GFDL-CM3). Similarly, Nome (Figure 11b) has a seasonally maritime climate and displays reductions of 32 and 27%, respectively. The above values for Anchorage and Nome are slightly higher than those found by O'Gorman (2014), which generally showed reductions of up to 30% for south and southwest Alaska when using a set of climate models from the CMIP5. Fairbanks (Figure 11c), with its cold continental climate, and Utqiaġvik (Figure 11d), located at high latitude and seasonally continental, do not show large changes in projected extreme snow amounts. These results for Fairbanks and Utqiaġvik are consistent with O'Gorman (2014) indicating that snowfall extremes tend to occur within a favourable temperature range that will continue to be realized in the Arctic, even under rapid warming. In both studies the reductions of mean snowfall are greater than are those for extreme snowfall.

Integrating all of the results found in this study and reconciling these against the historical climate model biases, it is evident that the historical overestimation of ACSNOW by CCSM4, combined with its unambiguous projection of ACSNOW decline (Figure 6, left) would lead to a much more rapid diminishment of snow in Alaska. CCSM4's historical positive (late) bias of spring snowmelt (Figure 8a, middle) makes sense given its overestimation of ACSNOW. The historical GFDL-CM3 shows a better agreement with the ERA-Interim with respect to ACSNOW (Figure 6, right), but it also generally shows a positive spring snowmelt bias (Figure 8a, bottom). The future projections from the GFDL-CM3 show a more rapid decline of ACSNOW and end-of-winter SWE than does CCSM4. This is possibly due to model differences of snow-albedo feedback; the GFDL-CM3 shows a greater reduction of surface albedo than does CCSM4 for mountainous areas as temperatures increase (Ghatak *et al.,* 2014). These snow-albedo disparities could also play a role in the historical differences discussed above. The GFDL-CM3 also indicates greater average warming across Alaska than the CCSM4 for the 21st-century according to the National Oceanic and Atmospheric Administration (NOAA) CMIP5 data visualization tool (http://www.esrl.noaa.gov/psd/ipcc/cmip5/).

5 | CONCLUSIONS

This study investigates projected changes of important snow season indicators for Alaska over 30-year periods (i.e., 1981–2010, 2011–2040, 2041–2070 and 2071–2100) using a combination of observations, downscaled reanalysis and climate model simulations. The dynamical downscaling provides finer spatial detail than previous research that analysed a set of CMIP5 models, and a more comprehensive set of variables than is made available from statistical downscaling. Total annual ACSNOW is projected to decrease in the future 30-year periods for all elevations at and below 2,000 m; however, low elevations (0–1,000 m) will likely experience more substantial decreases. This difference

results from increased ACSNOW during the core winter months at high elevations. All elevations below 1,000 m show reduced end-of-winter (April 1) SWE with each successive 30-year period.

The full-century projections of snow onset and snowmelt dates show trends that are 2–5 times higher than recently observed. However, modelled trends between the early-century period (2011–2040) and the historical are similar. These trends are especially important for spring soil recharge, which utilizes snowmelt water almost exclusively. Furthermore, despite projected ACSNOW increases at high elevations during the coldest months and no apparent changes to extreme ACSNOW at Fairbanks and Utqiaġvik, the periods outside of these months show large ACSNOW reductions. With continued warming in the coldest months beyond the periods in this study, it is plausible that all locations will eventually experience reduced mean and extreme ACSNOW, regardless of latitude or elevation.

ACKNOWLEDGEMENTS

Support for this work was provided by the National Science Foundation, Office of Polar Programs through Grant PLR-1268350 and by the NOAA Climate Program Office through Grant NA16OAR4310162 to the Alaska Center for Climate Assessment and Policy. The project described in this publication was supported by Cooperative Agreement No. G17AC00213 from the United States Geological Survey. Its contents are solely the responsibility of the authors and do not necessarily represent the views of the Alaska Climate Adaptation Science Center or the USGS. This manuscript is submitted for publication with the understanding that the United States Government is authorized to reproduce and distribute reprints for Governmental purposes. This work was supported in part by the high-performance computing and data storage resources operated by the Research Computing Systems Group at the University of Alaska Fairbanks, Geophysical Institute. We thank the two anonymous reviewers for their insightful and constructive comments.

ORCID

Rick Lader https://orcid.org/0000-0001-6365-6507

REFERENCES

Adam, J.C. and Lettenmaier, D.P. (2003) Adjustment of global gridded precipitation for systematic bias. *Journal of Geophysical Research*, 108(D9), 4257. https://doi.org/10.1029/2002/JD002499.

AMAP. (2017) *Snow, Water, Ice and Permafrost Summary. Summary for Policy-makers*. Oslo, Norway: Arctic Monitoring and Assessment Programme (AMAP), p. 20.

Beniston, M., Farinotti, D., Stoffel, M., Andreassen, L.M., Coppola, E., Eckert, N., Fantini, A., Giacona, F., Hauck, C., Huss, M., Huwald, H., Lehning, M., López-Moreno, J.-I., Magnussen, J., Marty, C., Morán-Tejéda, E., Morin, S., Naaim, M., Provenzale, A., Rabatel, A., Six, D., Stötter, J., Strasser, U., Terzago, S. and Vincent, C. (2018) The European mountain cryosphere: a review of its current state, trends, and future challenges. *The Cryosphere*, 12, 759–794. https://doi.org/10.5194/tc-12-759-2018.

Bieniek, P.A., Bhatt, U.S., Thoman, R.L., Angeloff, H., Partain, J., Papineau, J., Fritsch, F., Holloway, E., Walsh, J.E., Daly, C., Shulski, M., Hufford, G., Hill, D.F., Calos, S. and Gens, R. (2012) Climate divisions for Alaska based on objective methods. *Journal of Applied Meteorology and Climatology*, 51, 1276–1289. https://doi.org/10.1175/JAMC-D-11-0168.1.

Bieniek, P.A., Bhatt, U.S., Walsh, J.E., Rupp, T.S., Zhang, J., Krieger, J.R. and Lader, R. (2016) Dynamical downscaling of ERA-Interim temperature and precipitation for Alaska. *Journal of Applied Meteorology and Climatology*, 55, 635–654. https://doi.org/10.1175/JAMC-D-15-0153.1.

Bieniek, P.A., Bhatt, U.S., Walsh, J.E., Lader, R., Griffith, B., Roach, J.K. and Thoman, R.L. (2018) Assessment of Alaska rain-on-snow events using dynamical downscaling. *Journal of Applied Meteorology and Climatology*, 57, 1847–1863. https://doi.org/10.1175/JAMC-D-17-0276.1.

Bintanja, R. and Selten, F.M. (2014) Future increases in Arctic precipitation linked to local evaporation and sea-ice retreat. *Nature*, 509, 479–482. https://doi.org/10.1038/nature13259.

Brown, J. and Romanovsky, V.E. (2008) Report from the international permafrost association: state of permafrost in the first decade of the 21st century. *Permafrost and Periglacial Processes*, 19, 255–260. https://doi.org/10.1002/ppp.618.

Brown, R.D. and Robinson, D.A. (2011) Northern Hemisphere spring snow cover variability and change over 1922–2010 including an assessment of uncertainty. *The Cryosphere*, 5, 219–229. https://doi.org/10.5194/tc-5-219-2011.

Clilverd, H.M., White, D.M., Tidwell, A.C. and Rawlins, M.A. (2011) The sensitivity of northern groundwater recharge to climate change: a case study of Northwest Alaska. *Journal of the American Water Resources Association*, 47, 1228–1240. https://doi.org/10.1111/j.1752-1688.2011.00569.x.

Cohen, J.L., Furtado, J.C., Barlow, M.A., Alexeev, V.A. and Cherry, J.E. (2012) Arctic warming, increasing snow cover and widespread boreal winter cooling. *Environmental Research Letters*, 7, 014007. https://doi.org/10.1088/1748-9326/7/1/014007.

Cox, C.J., Stone, R.S., Douglas, D.C., Stanitski, D.M., Divoky, G.J., Dutton, G.S., Sweeney, C., George, J.C. and Longenecker, D.U. (2017) Drivers and environmental responses to the changing annual snow cycle of northern Alaska. *Bulletin of the American Meteorological Society*, 98, 2559–2577. https://doi.org/10.1175/BAMS-D-16-0201.1.

Danco, J.F., DeAngelis, A.M., Raney, B.K. and Broccoli, A.J. (2016) Effects of a warming climate on daily snowfall events in the Northern Hemisphere. *Journal of Climate*, 29, 6295–6318. https://doi.org/10.1175/JCLI-D-15-0687.1.

Dee, D.P., Uppala, S.M., Simmons, A.J., Berrisford, P., Poli, P., Kobayashi, S., Andrae, U., Balmaseda, M.A., Balsamo, G., Bauer, P., Bechtold, P., Beljaars, A.C.M., van de Berg, L., Bidlot, J., Bormann, N., Delsol, C., Dragani, R., Fuentes, M., Geer, A.J., Haimberger, L., Healy, S.B., Hersbach, H., Hólm, E.V., Isaksen,

L., Kållberg, P., Köhler, M., Matricardi, M., McNally, A.P., Monge-Sanz, B.M., Morcrette, J.-J., Park, B.-K., Peubey, C., de Rosnay, P., Tavolato, C., Thépaut, J.-N. and Vitart, F. (2011) The ERA-Interim reanalysis: configuration and performance of the data assimilation system. *Quarterly Journal of the Royal Meteorological Society*, 137, 553–597. https://doi.org/10.1002/qj.828.

Derksen, C., Brown, R., Mudryk, L. and Luojus, K. (2016) Terrestrial Snow Cover [in Arctic Report Card 2016], http://www.arctic.noaa.gov/Report-Card.

Donner, L.J., Wyman, B.L., Hemler, R.S., Horowitz, L.W., Ming, Y., Zhao, M., Golaz, J.-C., Ginoux, P., Lin, S.-J., Schwarzkopf, M.D., Austin, J., Alaka, G., Cooke, W.F., Delworth, T.L., Freidenreich, S. M., Gordon, C.T., Griffies, S.M., Held, I.M., Hurlin, W.J., Klein, S.A., Knutson, T.R., Langenhorst, A.R., Lee, H.-C., Lin, Y., Magi, B.I., Malyshev, S.L., Milly, P.C.D., Naik, V., Nath, M.J., Pincus, R., Ploshay, J.J., Ramaswamy, V., Seman, C.J., Shevliakova, E., Sirutis, J.J., Stern, W.F., Stouffer, R.J., Wilson, R.J., Winton, M., Wittenburg, A.T. and Zeng, F. (2011) The dynamical core, physical parameterizations, and basic simulation characteristics of the atmosphere component AM3 of the GFDL global coupled model CM3. *Journal of Climate*, 24, 3484–3519. https://doi.org/10.1175/2011JCLI3955.1.

Drusch, M.D., Vasiljevic, D. and Viterbo, P. (2004) ECMWF's global snow analysis: assessment and revision based on satellite observations. *Journal of Applied Meteorology*, 43, 1282–1294. https://doi.org/10.1175/1520-0450(2004)043<1282:EGSAAA>2.0.CO;2.

Dussault, C., Ouellet, J.-P., Courtois, R., Huot, J., Breton, L. and Jolicoeur, H. (2005) Linking moose habitat selection to limiting factors. *Ecography*, 28, 619–628. https://doi.org/10.1111/j.2005.0906-7590.04263.x.

ESA (2014) The third GlobSnow-2 newsletter gives an overview of the GlobSnow-2 SE and SWE v2.0 datasets released mid-December 2013, http://www.globsnow.info/index.php?page=Newsletters.

Estilow, T.W., Young, A.H. and Robinson, D.A. (2015) A long-term Northern Hemisphere snow cover extent data record for climate studies and monitoring. *Earth System Science Data*, 7, 137–142. https://doi.org/10.5194/essd-7-137-2015.

Frei, P., Kotlarski, S., Liniger, M.A. and Schär, C. (2018) Future snowfall in the Alps: projections based on the EURO-CORDEX regional climate models. *The Cryosphere*, 12, 1–24. https://doi.org/10.5194/tc-12-1-2018.

Ghatak, D., Sinsky, E. and Miller, J. (2014) Role of snow-albedo feedback in higher elevation warming over the Himalayas, Tibetan Plateau and Central Asia. *Environmental Research Letters*, 9, 114008. https://doi.org/10.1088/1748-9326/9/11/114008.

Hall, A. (2004) The role of surface albedo feedback in climate. *Journal of Climate*, 17, 1550–1568. https://doi.org/10.1175/1520-0442(2004)017<1550:TROSAF>2.0.CO;2.

Hinzman, L.D., Bettez, N.D., Bolton, W.R., Chapin, F.S., Dyurgerov, M.B., Fastie, C.L., Griffith, B., Hollister, R.D., Hope, A., Huntington, H.P., Jensen, A.M., Jia, G.J., Jorgenson, T., Kane, D. L., Klein, D.R., Kofinas, G., Lynch, A.H., Lloyd, A.H., McGuire, A.D., Nelson, F.E., Oechel, W.C., Osterkamp, T.E., Racine, C.H., Romanovsky, V.E., Stone, R.S., Stow, D.A., Sturm, M., Tweedie, C.E., Vourlitis, G.L., Walker, M.D., Walker, D.A., Webber, P.J., Welker, J.M., Winkler, K.S. and Yoshikawa, K. (2005) Evidence and implications of recent climate change in northern Alaska and other arctic regions. *Climatic Change*, 72, 251–298. https://doi.org/10.1007/s10584-005-5352-2.

IPCC. (2013) In: Stocker, T.F. , Qin, D. , Plattner, G.-K. , Tignor, M. , Allen, S.K. , Boschung, J. , Nauels, A. , Xia, Y. , Bex, V. and Midgley, P.M. (Eds.) *Climate Change 2013: The Physical Science Basis. Contribution of Working Group I to the Fifth Assessment Report of the Intergovernmental Panel on Climate Change*. Cambridge, United Kingdom and New York, NY: Cambridge University Press, p. 1535. https://doi.org/10.1017/CBO9781107415324.

Jeong, D.I., Sushama, L. and Khaliq, M.N. (2017) Attribution of spring snow water equivalent (SWE) changes over the northern hemisphere to anthropogenic effects. *Climate Dynamics*, 48, 3645–3658. https://doi.org/10.1007/s00382-016-3291-4.

Klein, G., Vitasse, Y., Rixen, C., Marty, C. and Rebetez, M. (2016) Shorter snow cover duration since 1970 in the Swiss Alps due to earlier snowmelt more than to later snow onset. *Climatic Change*, 139, 637–649. https://doi.org/10.1007/s10584-016-1806-y.

Kotlarski, S., Bosshard, T., Lüthi, D., Pall, P. and Schär, C. (2012) Elevation gradients of European climate change in the regional climate model COMSO-CLM. *Climatic Change*, 112, 189–215. https://doi.org/10.1007/s10584-011-0195-5.

Krasting, J.P., Broccoli, A.J., Dixon, K.W. and Lanzante, J.R. (2013) Future changes in Northern Hemisphere snowfall. *Journal of Climate*, 26, 7813–7828. https://doi.org/10.1175/JCLI-D-12-00832.1.

Kunreuther, H., Gupta, S., Bosetti, V., Cooke, R., Dutt, V., Ha-Duong, M., Held, H., Llanes-Regueiro, J., Patt, A., Shittu, E. and Weber, E. (2014) Integrated risk and uncertainty assessment of climate change response policies. In: Edenhofer, O. , Pichs-Madruga, R. , Sokona, Y. , Farahani, E. , Kadner, S. , Seyboth, K. , Adler, A. , Baum, I. , Brunner, S. , Eickemeier, P. , Kriemann, B. , Savolainen, J. , Schlömer, S. , von Stechow, C. , Zwickel, T. and Minx, J.C. (Eds.) *Climate Change 2014: Mitigation of Climate Change. Contribution of Working Group III to the Fifth Assessment Report of the Intergovernmental Panel on Climate Change*. Cambridge, United Kingdom and New York, NY: Cambridge University Press.

Lader, R., Bhatt, U.S., Walsh, J.E. and Rupp, T.S. (2016) Two-meter temperature and precipitation from atmospheric reanalysis evaluated for Alaska. *Journal of Applied Meteorology and Climatology*, 55, 901–922. https://doi.org/10.1175/JAMC-D-15-0162.1.

Lader, R., Walsh, J.E., Bhatt, U.S. and Bieniek, P.A. (2017) Projections of twenty-first-century climate extremes for Alaska via dynamical downscaling and quantile mapping. *Journal of Applied Meteorology and Climotology*, 56, 2393–2409. https://doi.org/10.1175/JAMC-D-16-0415.1.

Lawrence, D.M. and Slater, A.G. (2010) The contribution of snow condition trends to future ground climate. *Climate Dynamics*, 34, 969–981. https://doi.org/10.1007/s00382-009-0537-4.

Lawrence, D.M., Slater, A.G. and Swenson, S.C. (2012) Simulation of present-day and future permafrost and seasonally frozen ground conditions in CCSM4. *Journal of Climate*, 25, 2207–2225. https://doi.org/10.1175/JCLI-D-11-00334.1.

Lindsay, R., Wensnahan, M., Schweiger, A. and Zhang, J. (2014) Evaluation of seven different atmospheric reanalysis products in the Arctic. *Journal of Climate*, 27, 2588–2606. https://doi.org/10.1175/JCLI-D-13-00014.1.

Liston, G.E. and Hiemstra, C.A. (2011) The changing cryosphere: Pan-Arctic snow trends (1979–2009). *Journal of Climate*, 24, 5691–5712. https://doi.org/10.1175/JCLI-D-11-00081.1.

Littell, J.S., McAfee, S.A. and Hayward, G.D. (2018) Alaska snowpack response to climate change: statewide snowfall equivalent and

snowpack water scenarios. *Water*, 10, 668. https://doi.org/10.3390/w10050668.

Marty, C., Schlögl, S., Bavay, M. and Lehning, M. (2017) How much can we save? Impact of different emission scenarios on future snow cover in the Alps. *The Cryosphere*, 11, 517–529. https://doi.org/10.5194/tc-11-517-2017.

McAfee, S.A., Guentchev, G. and Eischeid, J.K. (2013a) Reconciling precipitation trends in Alaska: 1. Station-based analyses. *Journal of Geophysical Research: Atmospheres*, 118, 7523–7541. https://doi.org/10.1002/jgrd.50572.

McAfee, S.A., Walsh, J. and Rupp, T.S. (2013b) Statistically downscaled projections of snow/rain partitioning for Alaska. *Hydrological Processes*, 28, 3930–3946. https://doi.org/10.1002/hyp.9934.

Melvin, A.M., Larsen, P., Boehlert, B., Neumann, J.E., Chinowsky, P., Espinet, X., Martinich, J., Baumann, M.S., Rennels, L., Bothner, A., Nicolsky, D.J. and Marchenko, S.S. (2016) Climate change damages to Alaska public infrastructure and the economics of proactive adaptation. *Proceedings of the National Academy of Sciences of the United States of America*, 114(2), E122–E131. https://doi.org/10.1073/pnas.1611056113.

Menne, M.J., Durre, I., Vose, R.S., Gleason, B.E. and Houston, T.G. (2012) An overview of the global historical climatology network-daily database. *Journal of Atmospheric and Oceanic Technology*, 29, 897–910. https://doi.org/10.1175/JTECH-D-11-00103.1.

NOAA, National Centers for Environmental Information (2018) Climate at a Glance: City Time Series, published April 2018, retrieved on April 23, 2018 from http://www.ncdc.noaa.gov/cag/.

O'Gorman, P. (2014) Contrasting responses of mean and extreme snowfall to climate change. *Nature*, 512, 416–418. https://doi.org/10.1038/nature13625.

Overland, J.E., Hanna, E., Hanssen-Bauer, I., Kim, S.-J., Walsh, J.E., Wang, M., Bhatt, U.S. and Thoman, R.L. (2016) Surface Air Temperature [in Arctic Report Card 2016], http://www.arctic.noaa.gov/Report-Card.

Pastick, N.J., Jorgenson, M.T., Wylie, B.K., Nield, S.J., Johnson, K.D. and Finley, A.O. (2015) Distribution of near-surface permafrost in Alaska: estimates of present and future conditions. *Remote Sensing of Environment*, 168, 301–315. https://doi.org/10.1016/j.rse.2015.07.019.

Peng, X., Zhang, T., Frauenfeld, O.W., Wang, K., Luo, D., Cao, B., Su, H., Jin, H. and Wu, Q. (2018) Spatiotemporal changes in active layer thickness under contemporary and projected climate in the Northern Hemisphere. *Journal of Climate*, 31, 251–266. https://doi.org/10.1175/JCLI-D-16.0721.1.

Peters, G.P., Andrew, R.M., Boden, T., Canadell, J.G., Ciais, P., Le Quéré, C., Marland, G., Raupach, M.R. and Wilson, C. (2013) The challenge to keep global warming below 2°C. *Nature Climate Change*, 3(1), 4–6.

Rennert, K.J., Roe, G., Putkonen, J. and Bitz, C.M. (2009) Soil thermal and ecological impacts of rain on snow events in the circumpolar Arctic. *Journal of Climate*, 22, 2302–2315. https://doi.org/10.1175/2008JCLI2117.1.

Riahi, K., Rao, S., Krey, V., Cho, C., Chirkov, V., Fischer, G., Kindermann, G., Nakicenovic, N. and Rafaj, P. (2011) RCP 8.5—a scenario of comparatively high greenhouse gas emissions. *Climatic Change*, 109, 33–57. https://doi.org/10.1007/s10584-011-0149-y.

Schmucki, E., Marty, C., Fierz, C. and Lehning, M. (2014) Simulations of 21st century snow response to climate change in Switzerland from a set of RCMs. *International Journal of Climatology*, 35, 3262–3273. https://doi.org/10.1002/joc.4205.

Skamarock, W.C., Klemp, J.B., Dudhia, J., Gill, D.O., Barker, D.M., Duda, M.G., Huang, X.-Y., Wang, W. and Powers, J.G. (2008) A description of the Advanced Research WRF version 3. NCAR Tech. Note NCAR/TN-475+STR, 113 pp., doi:10.1056/D68S4MVH.

Strasser, U. (2008) Snow loads in a changing climate: new risks? *Natural Hazards and Earth System Sciences*, 8, 1–8.

Sun, F., Hall, A., Schwartz, M., Walton, D.B. and Berg, N. (2016) Twenty-first century snowfall and snowpack changes over the Southern California mountains. *Journal of Climate*, 29, 91–110. https://doi.org/10.1175/JCLI-D-15-0199.1.

Taylor, K.E., Stouffer, R.J. and Meehl, G.A. (2012) An overview of CMIP5 and the experiment design. *Bulletin of the American Meteorological Society*, 93, 485–498. https://doi.org/10.1175/BAMS-D-11-00094.1.

Walsh, J.E., Chapman, W.L., Romanovsky, V., Christensen, J.H. and Stendel, M. (2008) Global climate model performance over Alaska and Greenland. *Journal of Climate*, 21, 6156–6174. https://doi.org/10.1175/2008JCLI2163.1.

Walter Anthony, K., Daanen, R., Anthony, P., Schneider von Deimling, T., Ping, C., Chanton, J.P. and Grosse, G. (2016) Methane emissions proportional to permafrost carbon thawed in Arctic lakes since the 1950s. *Nature Geoscience*, 9, 679–682. https://doi.org/10.1038/ngeo2795.

Wang, M. and Overland, J.E. (2015) Projected future duration of the sea-ice-free season in the Alaskan Arctic. *Progress in Oceanography*, 136, 50–59. https://doi.org/10.1016/j.pocean.2015.01.001.

Wendler, G. and Shulski, M. (2009) A century of climate change for Fairbanks, Alaska. *Arctic*, 62, 295–300.

Yang, D., Goodison, B.E., Metcalfe, J.R., Golubev, V.S., Bates, R., Pangburn, T. and Hanson, C.L. (1998a) Accuracy of NWS 8 standard nonrecording precipitation gauge: results and application of WMO Intercomparison. *Journal of Atmospheric and Oceanic Technology*, 15, 54–68. https://doi.org/10.1175/1520-0426(1998)015<0054:AONSNP>2.0.CO;2.

Yang, D., Goodison, B.E. and Ishida, S. (1998b) Adjustment of daily precipitation data at 10 climate stations in Alaska: application of World Meteorological Organization Intercomparison results. *Water Resources Research*, 34, 241–256. https://doi.org/10.1029/97WR02681.

Young-Robertson, J.M., Bolton, W.R., Bhatt, U.S., Cristóbal, J. and Thoman, R. (2016) Deciduous trees are a large and overlooked sink for snowmelt water in the boreal forest. *Scientific Reports*, 6, 29504. https://doi.org/10.1038/srep29504.

Zhang, X., He, J., Zhang, J., Polyakov, I., Gerdes, R., Inoue, J. and Wu, P. (2012) Enhanced poleward moisture transport and amplified northern high-latitude wetting trend. *Nature Climate Change*, 3, 47–51. https://doi.org/10.1038/nclimate1631.

How to cite this article: Lader R, Walsh JE, Bhatt US, Bieniek PA. Anticipated changes to the snow season in Alaska: Elevation dependency, timing and extremes. *Int J Climatol*. 2019;1–19. https://doi.org/10.1002/joc.6201